



Article

# Mistletoe-Extract Drugs Stimulate Anti-Cancer V $\gamma$ 9V $\delta$ 2 T Cells

Ling Ma<sup>1,2</sup>, Swati Phalke<sup>1,2</sup> , Caroline Stévigny<sup>3</sup>, Florence Souard<sup>1,4</sup>   
and David Vermijlen<sup>1,2,\*</sup>

<sup>1</sup> Department of Pharmacotherapy and Pharmaceutics, Université Libre de Bruxelles (ULB), 1050 Bruxelles, Belgium; ling.ma@ulb.ac.be (L.M.); swatiphalk08@gmail.com (S.P.); Florence.Souard@ulb.be (F.S.)

<sup>2</sup> Institute for Medical Immunology, Université Libre de Bruxelles (ULB), 6041 Gosselies, Belgium

<sup>3</sup> RD3 Department-Unit of Pharmacognosy, Bioanalysis and Drug Discovery, Université Libre de Bruxelles (ULB), 1050 Bruxelles, Belgium; Caroline.Stevigny@ulb.be

<sup>4</sup> DPM UMR 5063, CNRS, Université Grenoble Alpes, 38041 Grenoble, France

\* Correspondence: David.Vermijlen@ulb.be

Received: 31 May 2020; Accepted: 23 June 2020; Published: 26 June 2020



**Abstract:** Human phosphoantigen-reactive V $\gamma$ 9V $\delta$ 2 T cells possess several characteristics, including MHC-independent recognition of tumor cells and potent killing potential, that make them attractive candidates for cancer immunotherapeutic approaches. Injectable preparations from the hemi-parasite plant *Viscum album* L. (European mistletoe) are commonly prescribed as complementary cancer therapy in European countries such as Germany, but their mechanism of action remains poorly understood. Here, we investigated in-depth the in vitro response of human T cells towards mistletoe-extract drugs by analyzing their functional and T-cell-receptor (TCR) response using flow cytometry and high-throughput sequencing respectively. Non-fermented mistletoe-extract drugs (AbnobaViscum), but not their fermented counterparts (Iscador), induced specific expansion of V $\gamma$ 9V $\delta$ 2 T cells among T cells. Furthermore, AbnobaViscum rapidly induced the release of cytotoxic granules and the production of the cytokines IFN $\gamma$  and TNF $\alpha$  in V $\gamma$ 9V $\delta$ 2 T cells. This stimulation of anti-cancer V $\gamma$ 9V $\delta$ 2 T cells was mediated by the butyrophilin BTN3A, did not depend on the accumulation of endogenous phosphoantigens and involved the same V $\gamma$ 9V $\delta$ 2 TCR repertoire as those of phosphoantigen-reactive V $\gamma$ 9V $\delta$ 2 T cells. These insights highlight V $\gamma$ 9V $\delta$ 2 T cells as a potential target for mistletoe-extract drugs and their role in cancer patients receiving these herbal drugs needs to be investigated.

**Keywords:** gammadelta; Vgamma9Vdelta2; herbal drug; mistletoe; T cell receptor; TCR

## 1. Introduction

Recently, T cell-based cancer immunotherapy has become a main therapy arm in the clinic besides surgery, radio- and chemotherapy. While mostly conventional  $\alpha\beta$  T cells are considered, it has become increasingly clear that  $\gamma\delta$  T cells have a large potential, which is illustrated by the interest of commercial partners [1]. The  $\gamma\delta$  T cells express a T cell receptor (TCR) on their cell surface that is composed of a  $\gamma$  and a  $\delta$  chain and the TCR-dependent recognition of cancer cells usually do not rely on classical MHC molecules. The antitumor function of  $\gamma\delta$  T cells is generally associated with their cytotoxic potential and their production of both interferon  $\gamma$  (IFN $\gamma$ ) and tumor necrosis factor  $\alpha$  (TNF $\alpha$ ) [1,2]. The  $\gamma\delta$  TCR is generated by the somatic recombination of the TRG and TRD loci, combining different variable (V), diversity (D, only in TRD), and joining (J) gene segments [3,4]. This combinational diversity together with junctional diversity can result in a large variation in possible V(D)J junctions, also called complementary-determining-region-3 (CDR3), the part of the

TCR that usually plays an important role in antigen recognition.  $\gamma\delta$  T cells can be divided into subsets based on the type of V gene segment used in their  $\gamma\delta$  TCR. A major  $\gamma\delta$  T cell population in adult human peripheral blood is represented by V $\gamma$ 9V $\delta$ 2 T cells that are defined by the expression of a TCR containing the  $\gamma$ -chain variable region 9 (V $\gamma$ 9, TRGV9) and the  $\delta$ -chain V region 2 (V $\delta$ 2, TRDV2). They are poised towards a cytotoxic type 1 effector phenotype: they can kill target cells through the degranulation of cytotoxic granules (containing perforin and granzymes) and they produce swiftly IFN $\gamma$  and TNF $\alpha$  upon activation [1]. V $\gamma$ 9V $\delta$ 2 T cells respond (expansion, release of cytotoxic granules, cytokine production) in a TCR-dependent manner towards small metabolites derived from the isoprenoid pathway, such as the endogenous-derived isopentenyl pyrophosphate (IPP) or the microbial-derived (E)-4-Hydroxy-3-methyl-but-2-enyl pyrophosphate (HMBPP), that critically depends on the transmembrane protein butyrophilin3A1 (BTN3A1) [5,6]. The V $\gamma$ 9V $\delta$ 2 T cell subset has been a target for cancer clinical trials, mainly through their in vivo activation via the administration of aminobisphosphonates such as zoledronate. Aminobisphosphonates inhibit the farnesyl pyrophosphate synthase enzyme (FPPS) leading to the intracellular accumulation of endogenous IPP [1,7]. Interestingly, V $\gamma$ 9V $\delta$ 2 T cells also respond to alkylamines such as *sec*-butylamine that are found in edible plants and tea [8,9]. These alkylamines, like aminobisphosphonates, activate V $\gamma$ 9V $\delta$ 2 T cells indirectly through inhibition of the FPPS enzyme [10]. The stimulation of the antitumor function of  $\gamma\delta$  T cells by such plant-derived compounds are thought to play an important role in the prevention of cancer development [11–13].

Injectable preparations from the hemi-parasite plant *Viscum album* L. (European mistletoe) are the most frequently prescribed complementary cancer therapy in central European countries. For example, in Germany, up to 77% of cancer patients apply this therapy in the context of integrative oncological approaches and thus belong to the most prescribed drugs offered to cancer patients [14–16]. Mistletoe extracts are prepared as aqueous solutions and they can either be fermented (e.g., Iscador) or unfermented (e.g., AbnobaViscum) [15,17]. In addition, the commercial products can be subdivided according to the species of host tree, which is typically indicated in the product name by a suffix letter, such as P for pini (pine) and M for mali (apple tree). The different types of preparations and different host trees may contribute to variable contents of biological active substances [15]. In vitro studies and animal tumor models have shown that mistletoe extracts can be cytotoxic and immunomodulatory, but their precise mode of action is poorly understood [15,17–19].

Mistletoe treatment has been suggested to increase the survival of cancer patients, but this is controversial and thus an increased understanding of its mechanism of action is needed to guide further in vivo studies and clinical trials [14,15,19]. Here we show that non-fermented mistletoe-extract drugs (AbnobaViscum) stimulate and expand specifically V $\gamma$ 9V $\delta$ 2 T cells, induce the release of cytotoxic granules and promote the production of the cytokines IFN $\gamma$  and TNF $\alpha$ . Furthermore, we show that this mistletoe-mediated activation of anti-cancer V $\gamma$ 9V $\delta$ 2 T cells is rapid and direct (i.e., not dependent on the accumulation of endogenous phosphoantigens) and is completely BTN3A-dependent.

## 2. Materials and Methods

### 2.1. Sample Collection

Peripheral blood mononuclear cells (PBMC) from healthy adult donors (> 18 years) were isolated from blood donations at the CHU Tivoli (La Louvière, Belgium) and included informed consent of the donors (Ethics Commission CHU Tivoli, ethical code number 917, 29 October 2013). The study was conducted in accordance with the Declaration of Helsinki. PBMC were isolated by Lymphoprep gradient centrifugation (AxisShield, Dundee, UK) and cryopreserved in liquid nitrogen.

### 2.2. Cell Culture and Treatments

PBMC were thawed at 37 °C in complete medium [(RPMI 1640 (Gibco, Invitrogen, Waltham, MA, USA), supplemented with L-glutamine (2 mM), penicillin (50 U/mL), streptomycin (50 U/mL),

and 1% nonessential amino acids (Lonza, Basel, Switzerland) and 10% (*v/v*) heat-inactivated FCS (PPA Laboratories, Hickory, NC, United States)] and cultured in 96-well round bottom plates at  $2 \times 10^5$  cells/well ( $1 \times 10^6$  cells/mL). For activation tests (CD69 and proliferation), PBMC were rested for 2 h or overnight after thawing, then the stimulating compounds were added at following concentrations: HMBPP (10 nM, Echelon Bioscience, Salt Lake City, UT, USA), zoledronate (1  $\mu$ M, Novartis, Basel, Switzerland), sec-butylamine (0.5 mM, Sigma-Aldrich, St. Louis, MO, USA), mistletoe extracts (1000  $\mu$ g/mL). AbnobaViscum Pini and AbnobaViscum Mali were obtained from Abnoba GmbH (Pforzheim, Germany) and Iscador Pinus and Iscador Malus from Iscador AG (Arlesheim, Switzerland). The stock concentration was for all mistletoe-extract drugs 20 mg/mL. Cells were cultured at 37 °C and 5% CO<sub>2</sub>. For the CD69 readout, the cells were cultured for 1 day and tested. For the proliferation assay, PBMC were either cultured in the presence of heat-treated mistletoe extracts for 7 days or washed 3 times after 1 day of incubation with non-heated extracts to remove stimulants (pulse stimulation), and then complete medium with 100 U/mL IL-2 was added (re-added at day 3 or day 4) and cultured for 7 days. Carboxyfluorescein succinimidyl ester (CFSE) labeling was done with CellTrace™ CFSE Cell Proliferation Kit (Thermo Fisher Scientific, Waltham, MA, USA): after resting, cells were labeled at a cell concentration of  $15 \times 10^6$  cells/mL and 1.5  $\mu$ M CFSE for 5 min at room temperature and washed 3 times after which the stimulators were added and the cells were cultured for 5 days. For the determination of cytokine production in T cells, no IL-2 were added during culture and 2  $\mu$ M monensin was added 4 h before harvest. For the CD107a assay: in the 4 h-stimulation assays, CD107a-PC7 (clone eBioH4A3, eBioscience) was added right after the addition of the stimulant, the cells were incubated for an hour after which monensin was added; in 1 day-stimulation assays, CD107a and monensin were added 4 h before harvesting the cells. For the assays with mevastatin, cells were pretreated with 2  $\mu$ M mevastatin (Sigma-Aldrich) for 1 h, then proceeded to stimulation and CD107a staining. For BTN3A blocking tests, zoledronate-expanded (1  $\mu$ M, 10–14 days, cryopreserved) PBMC were used to restimulate with the indicated stimulants. BTN3A (clone 103.2, kind gift from Imcheck Therapeutics; final concentration was 10  $\mu$ g/mL) [20] and isotype control (IgG2A, 10  $\mu$ g/mL) antibodies were added 1 h before stimulation. For apyrase (Sigma-Aldrich) treatment, each stimulant was incubated with 0.2 U/mL at 37 °C for 2 h, control stimulants were incubated at 37 °C for 2 h without apyrase. For heat treatment, mistletoe products were heated at 80 °C for 5 min.

### 2.3. Flow Cytometry and Antibody Reagents

Harvested cells were first washed with PBS, then labeled with 1000 times diluted Zombie NIR™ dye (Biolegend, San Diego, CA, USA) at room temperature for 20 min and washed with 0.1%BSA/PBS. For surface staining, cells were incubated with antibody mix at 4 °C for 15–20 min, then washed and resuspended with 1%PFA/PBS. For intracellular cytokine stainings, after surface staining, CytofixCytoperm™ (BD) was used to permeabilize cell membranes. Staining results were acquired either on CyAn ADP cytometer (Dako Cytomation) or LSRFortessa (BD); analysis was done using FlowJo software and R.

The following antibodies were used in this study: CD3-PB (clone UCHT1, BD), CD3-BV510 (UCHT1, BD), TCR  $\gamma\delta$ -APC (11F2, Miltenyi Biotec, Bergisch Gladbach, Germany), TCR V $\gamma$ 9-PC5 (IMMU 360, Beckman Coulter, Brea, CA, USA), TCR V $\delta$ 2-FITC (IMMU 389, Beckman Coulter), CD4-V500 (RPA-T4, BD), CD4-BV510 (RPA-T4, BD), CD8-PC7 (SFCI21Thy2D3, Beckman Coulter), CD56-PE-CF594 (NCAM16.2, BD), CD69-PE (FN50, BD), IFN $\gamma$ -V450 (B27, BD), TNF $\alpha$ -FITC (MAB11, BD), IL-17a-PE (eBio64DEC17, eBioscience). Dead cells were excluded (negative for Zombie NIR) and gated on CD3+ lymphocytes (Supplementary Figure S1). Gating CD3+V $\gamma$ 9+ lymphocytes identify the vast majority of V $\gamma$ 9V $\delta$ 2 T cells in adult blood [21].

### 2.4. Cell Sorting, RNA Isolation, and CDR3 Analysis

PBMC were exposed to 10 nM HMBPP, 1  $\mu$ M zoledronate, and 1000  $\mu$ g/mL AbnobaViscum P for 1 day, washed 3 times, after which complete medium containing 100 U/mL IL-2 was added. IL-2 was

added every 3–4 days during culturing for 14 days to allow an expansion of V $\gamma$ 9V $\delta$ 2 T cells. Harvested cells were labeled with Zombie NIR™ dye (Biolegend) at room temperature for 10 min, and stained with CD3/TCR- $\gamma\delta$ /TCR-V $\gamma$ 9/TCR-V $\delta$ 2 antibodies at 4 °C for 15 min. Zombie NIR-CD3+ $\gamma\delta$ +V $\gamma$ 9+ V $\delta$ 2+ T cells were sorted on FACS Aria III (BD) (purity range 94.4–100% (%V $\gamma$ 9V $\delta$ 2 of T cells)). Cells were snap-frozen in liquid nitrogen and preserved at –80 °C.

RNA was isolated from sorted cells (~10000 cells each sample) with the RNeasy Micro Kit (Qiagen, Hilden, Germany) and CDR3 $\gamma$  and CDR3 $\delta$  high-throughput sequencing was performed as described before [22]. Briefly, RNA was reverse transcribed via a template-switch cDNA reaction followed by a PCR amplifying the CDR3 $\gamma$  and CDR3 $\delta$  regions. High-throughput sequencing of the generated amplicon products containing the TRG and TRD sequences was performed on an Illumina MiSeq platform using the V2 300 kit, with 150 base pairs (bp) at the 3' end (read 2) and 150 bp at the 5' end (read 1) [at the GIGA center, University of Liège, Belgium]. Raw sequencing reads from fastq files (read 1 and read 2) were past the quality check using fastqc (version 0.11.8, <http://www.bioinformatics.babraham.ac.uk/projects/fastqc/>). Then the sequences were aligned to reference V, D, and J genes from GenBank database specifically for 'TRG' or 'TRD' to build CDR3 sequences using the MiXCR software (version 3.0.3) [23]. Default parameters were used except to assemble TRDD gene segment where 3 instead of 5 consecutive nucleotides were applied as an assemble parameter. CDR3 sequences were then exported and analyzed using VDJtools software (version 1.2.1) using default settings [24]. Data for CDR3 length, treemaps and (D)J usage are generated by the VDJtools routine 'annotate'; normalized Shannon Wiener Index by the routine 'CalcDiversityStats'; Top shared clonotypes by the routine 'TrackClonotypes' and multidimensional scaling analyzing by the routine 'ClusterSamples' [24]. Sequences that were out of frame and contained stop codons were excluded from the analysis. Files generated from VDJtools were uploaded into Rstudio (version 1.1.463, R version 3.5.2) and analysis involving the following packages: Treemap (<https://CRAN.R-project.org/package=treemap>) to generate Treemap plots, ggplot2 [25] for data visualization and ggpubr (<https://CRAN.R-project.org/package=ggpubr>) for statistical analysis.

### 2.5. Data Availability

Fastq files of TRG and TRD sequences are deposited under SRA accession code PRJNA633174.

### 2.6. Statistics

Statistical analysis was performed with the R software package ggpubr (<https://CRAN.R-project.org/package=ggpubr>). Paired t-test was used for normally (determined by the Shapiro-Wilk test,  $p > 0.05$ ) distributed data and with equal variances (determined by the Levene's test,  $p > 0.05$ ). Otherwise, Wilcoxon signed-rank test was used.

## 3. Results

### 3.1. *AbnobaViscum* but Not *Iscador* Mistletoe Extracts Induce Specific Expansion of V $\gamma$ 9V $\delta$ 2 T Cells

We obtained four commercially available *Viscum album* L. (VA) extracts from two companies that derive them from the same host trees but use different preparatory methods: non-fermented extracts are *AbnobaViscum* Pini (AP) and *AbnobaViscum* Mali (AM) and fermented products are *Iscador* Malus (IM) and *Iscador* Pinus (IP). In order to perform short-term (4 h, 1 day) assays to assess T cell activation (CD69) and function (cytokine production and release of cytotoxic granules) and long-term (7 days) expansion cultures, we first titrated each extract to assess the potential cytotoxic effect and dose-response in PBMC cultures. After 1 day of culture, none of the extracts showed a cytotoxic effect (Supplementary Figure S2A, left panels). At 7 days however, all the VA extracts except IP showed a clear dose-dependent cytotoxicity (Supplementary Figure S2A, right panels). Heat treatment of mistletoe extracts [26] prevented the cell death induction in the long-term PBMC cultures (Supplementary Figure S2B). As heat-treatment is not performed on the mistletoe-extracts that are

injected in cancer patients, we preferred to test an alternative method to prevent the cytotoxic effects in order to verify whether the heat-treatment was essential for possible effects on V $\gamma$ 9V $\delta$ 2 T cells [26]. Exposure of the cells for one day to the VA extracts (at the highest concentration, 1000  $\mu$ g/mL) followed by washing ('pulse'), instead of continued exposure, prevented or reduced significantly the cytotoxic effects in longer term cultures (Supplementary Figure S2B). Thus, we included results from both heat treatment and pulse stimulation in the 7 days expansion cultures since both methods resulted in similar expansion levels (%V $\gamma$ 9+ of CD3+ T cells, data not shown). Based on short-term activation experiments with the lymphocyte activation marker CD69, we selected 1000  $\mu$ g/mL concentration of mistletoe extracts for further experiments (Supplementary Figure S3). Both AbnobaViscum (AP and AM) and Iscador (IA and IM) VA extracts activated V $\gamma$ 9+  $\gamma$  $\delta$  T cells, with no or minimal effects on V $\gamma$ 9- $\gamma$  $\delta$  T cells and  $\alpha\beta$  T cells (Figure 1A). A different trend was observed for NK cells: here the activation was more pronounced with Iscador compared to AbnobaViscum extracts (Figure 1A). Surprisingly, while both AbnobaViscum and Iscador extracts activated V $\gamma$ 9V $\delta$ 2 T cells (Figure 1A), and despite being derived from the same host trees, only AbnobaViscum extracts induced proliferation of V $\gamma$ 9V $\delta$ 2 T cells (Figure 1B,C). AP was the strongest stimulant (Figure 1C; AP vs AM:  $p = 0.0078$ , Wilcoxon signed-rank test) and the expansion was highly restricted to V $\gamma$ 9V $\delta$ 2 T cells (Figure 1B for CD3+ T cells, data not shown for CD3- NK cells). We therefore focused further on the stimulation of V $\gamma$ 9V $\delta$ 2 upon treatment with AP. Of note, AP-induced expansion levels were similar to expansion levels observed with known V $\gamma$ 9V $\delta$ 2 T cell stimulants (HMBPP, zoledronate) and individual AP-, HMBPP-, and zoledronate-induced expansions showed a strong correlation (Figure 1D).

In sum, although both AbnobaViscum (non-fermented) and Iscador (fermented) VA extracts can activate V $\gamma$ 9V $\delta$ 2 T cells, only exposure to AbnobaViscum VA extracts results in their proliferation. This strong expansion was highly specific for V $\gamma$ 9V $\delta$ 2 T cells.

### 3.2. AbnobaViscum Rapidly Stimulates the Release of Cytotoxic Granules and the Production of IFN $\gamma$ and TNF $\alpha$ in V $\gamma$ 9V $\delta$ 2 T Cells

As VA-extract drugs are used as complementary cancer therapy, we assessed the induction of the two main anti-cancer functions of V $\gamma$ 9V $\delta$ 2 T cells: degranulation of their cytotoxic granules (by analyzing the surface expression of the granule-associated CD107a) and the induction of the cytokines IFN $\gamma$  and TNF $\alpha$ . AP induced a rapid (4 h) and striking upregulation of CD107a, IFN $\gamma$  and TNF $\alpha$  in V $\gamma$ 9+ T cells, but not on V $\gamma$ 9- T cells (Figure 2A–D). The release of cytotoxic granules and production of cytokines were largely co-expressed (Figure 2D). While some studies have ascribed an anti-tumor role for IL-17-producing  $\gamma$  $\delta$  T cells like when they act in concert with immunogenic cell death-inducing chemotherapeutic drugs [27], in a range of other settings a pro-tumor role has been proposed [1,2,28]. Here, we could not find significant upregulation of this cytokine in V $\gamma$ 9V $\delta$ 2 T cells upon exposure to AP (Supplementary Figure S4). Of note, the stimulation kinetics of AP (4 h rather than 1 day) was similar to the stimulation kinetics of HMBPP (direct activation) but not with the kinetics of the indirect stimulatory compounds zoledronate and *sec*-butylamine (Figure 2E). In sum, AP rapidly stimulates the degranulation of cytotoxic granules and the production of the anti-cancer cytokines IFN $\gamma$  and TNF $\alpha$  in V $\gamma$ 9V $\delta$ 2 T cells but not within other T cells.



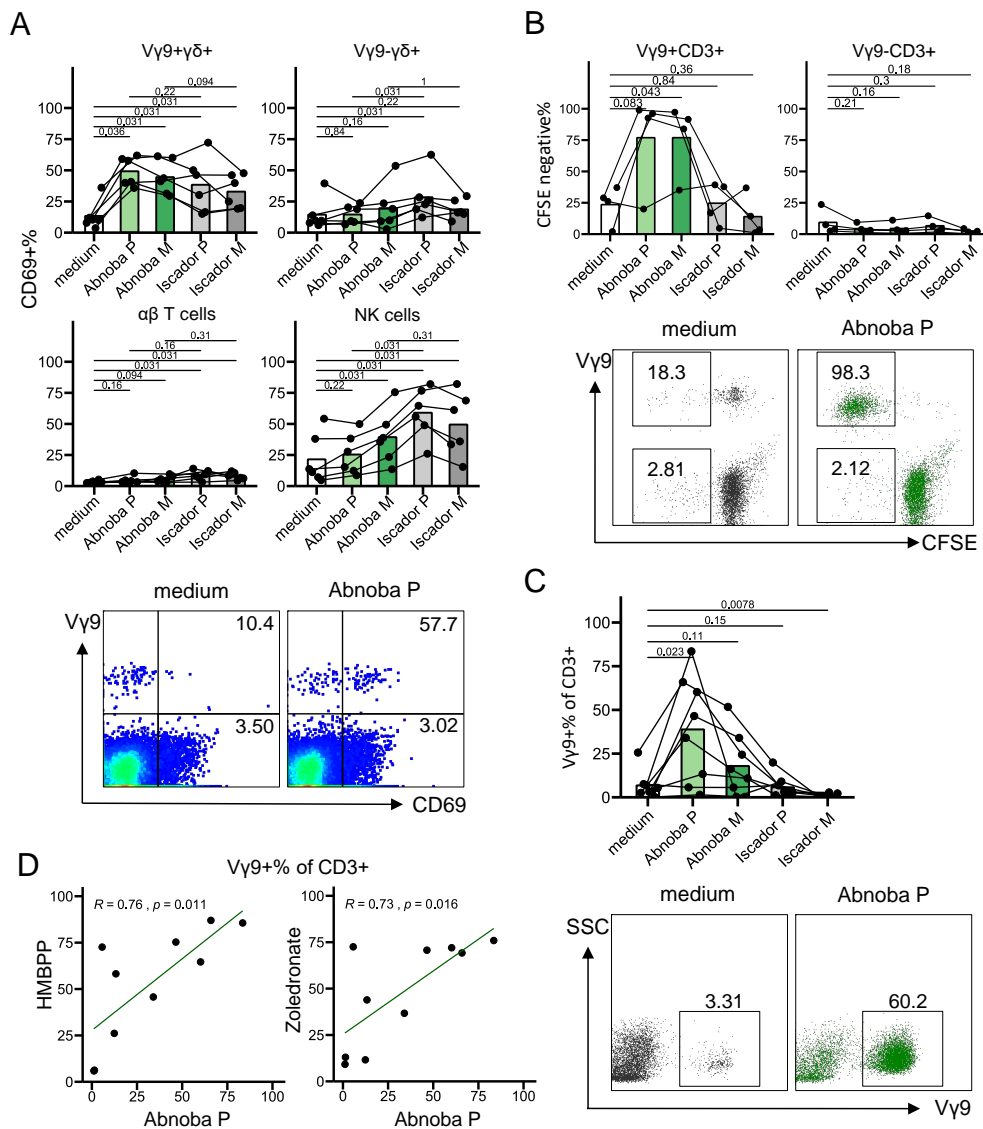


**Figure 1.** AbnobaViscum but not Iscador mistletoe extracts induce specific expansion of Vγ9Vδ2 T cells. (A) Percentage of CD69 expression on different cell types after stimulation with different mistletoe extracts for 1 day. Upper left: Vγ9+ γδ T cells (CD3+γδ+Vγ9+); upper right: Vγ9- γδ T cells (CD3+γδ+Vγ9-); lower left: αβ T cells (CD3+γδ-); lower right: natural killer (NK) cells (CD3-CD56+). Lines connect the same subjects (n = 6), bars indicate mean values. Values on the graphs indicate p values (obtained with the Wilcoxon signed-rank test). Bottom panels show representative flow cytometry plots (gated on CD3+ T cells), numbers indicate percentages of CD69+ cells, expressed as a percentage of Vγ9+CD3+ cells (top) and as a percentage of Vγ9-CD3+ cells (bottom). (B) Percentage of CFSE-negative Vγ9+ T cells (CD3+Vγ9+, upper left) and Vγ9- T cells (CD3+Vγ9-, upper right) after stimulation for 5 days with different mistletoe extracts. Lines connect the same subjects (n = 4), bars indicate mean values. Values on the graphs indicate p values (obtained with the paired T-test). Bottom panels show representative flow cytometry plots (gated on CD3+ T cells), numbers indicate percentages of CFSE-negative cells, expressed as a percentage of Vγ9+CD3+ (top) and as a percentage of Vγ9-CD3+ (bottom). (C) Percentage of Vγ9+ cells (of total CD3+ T cells) after stimulated with different mistletoe extracts for 7 days. Lines connect the same subjects (n = 8), bars indicate mean values. Values on the graphs indicate p values (obtained with the Wilcoxon signed-rank test). Bottom panels show representative flow cytometry plots (gated on CD3+ T cells), numbers indicate percentages of positive cells in the indicated gates. (D) Correlation between AbnobaViscum P- and HMBPP-, and zoledronate-induced expansion (7 days). Each dot represents one subject (n = 10).

### 3.3. *AbnobaViscum* Stimulation of $V\gamma 9V\delta 2$ T Cells is Direct and *BTN3A*-Dependent

Alkylamines such as *sec*-butylamine of edible plants and tea have been described as main  $V\gamma 9V\delta 2$  T cell-stimulating compounds [8,9] and to act, like aminobisphosphonates, indirectly by endogenous phosphoantigen (IPP) accumulation (10). Whether the same kind of 'indirect'  $V\gamma 9V\delta 2$  activating compounds or rather more direct mechanism are involved in the AP-induced activation is not clear. In order to verify the involvement of endogenous accumulation of IPP we used mevastatin, to inhibit HMG-Coenzyme A reductase activity upstream of IPP synthesis and thus to inhibit IPP production [29]. To our surprise, inhibiting IPP synthesis did not decrease the AP-induced stimulation (Figure 3A). As expected, direct HMBPP-induced activation was not influenced by mevastatin treatment as well, while *sec*-butylamine- and zoledronate-induced  $V\gamma 9V\delta 2$  T cell activation were inhibited (Figure 3A). These results rather indicate that AP contains (a) direct activating pyrophosphate compound(s). To address this further, pretreatment of AP with apyrase, that sequentially releases inorganic phosphate groups from phosphorylated molecules, completely abolished the  $V\gamma 9V\delta 2$  T cell response, while the same pretreatment of zoledronate and *sec*-butylamine did not influence their  $V\gamma 9V\delta 2$  T cell-activation potential (Figure 3B). To investigate further the mechanism of activation of  $V\gamma 9V\delta 2$  T cells by AP, we verified the involvement of *BTN3A*, that plays a crucial role in the phosphoantigen-mediated activation via the  $V\gamma 9V\delta 2$  TCR: the blocking *BTN3A* antibody 103.2 completely abolished AP-induced degranulation and cytokine production (Figure 3C). Thus overall, the AP-induced activation of  $V\gamma 9V\delta 2$  T cells does not depend on the accumulation of endogenous IPP production and is mediated via *BTN3A*.

### 3.4. The *AbnobaViscum*-Responsive $V\gamma 9V\delta 2$ TCR Repertoire is Similar to the Phosphoantigen-Responsive Repertoire

Next, we wondered whether the *BTN3A*/ $V\gamma 9V\delta 2$  TCR-dependent AP stimulation induces a similar polyclonal  $V\gamma 9V\delta 2$  T cell response as HMBPP and zoledronate [30] or whether AP targets rather a subset of  $V\gamma 9V\delta 2$  T cells. In order to address this issue, we investigated the CDR3 $\gamma$  and CDR3 $\delta$  repertoire by high-throughput sequencing of  $V\gamma 9V\delta 2$  T cells expanded with AP, and compared it to HMBPP- and zoledronate-expanded  $V\gamma 9V\delta 2$  T cells. The CDR3 length distributions were highly similar between AP-, HMBPP- and zoledronate-expanded  $V\gamma 9V\delta 2$  T cells (Figure 4A). Compared to HMBPP- and zoledronate- expanded  $V\gamma 9V\delta 2$  T cells, AP-expanded CDR3 $\gamma$  and CDR3 $\delta$  sequences showed the same diversity levels (Figure 4B), the same TRGJ and TRDJ usage (Figure 4C) and were highly shared (Figure 4D). This high sharing between the different treatments was mainly due to public clonotypes in the TRGV9 repertoire, i.e., shared between the different individuals (Figure 4D, left panels), while the shared AP/HMBPP/zoledronate TRDV2 repertoire was private for each individual (Figure 4D, right panels). This was further shown by a global analysis via multidimension scaling (MDS): the AP-, HMBPP- and zoledronate-expanded TRD repertoire were grouped in subject-based clusters (Figure 4E, right panel), highlighting again the similarities between the  $V\gamma 9V\delta 2$  TCR responses induced by AP, HMBPP and zoledronate.

In sum, the AP-responsive  $V\gamma 9V\delta 2$  TCR repertoire is similar to the direct (HMBPP) and indirect (zoledronate-induced IPP accumulation) phosphoantigen-responsive repertoire.

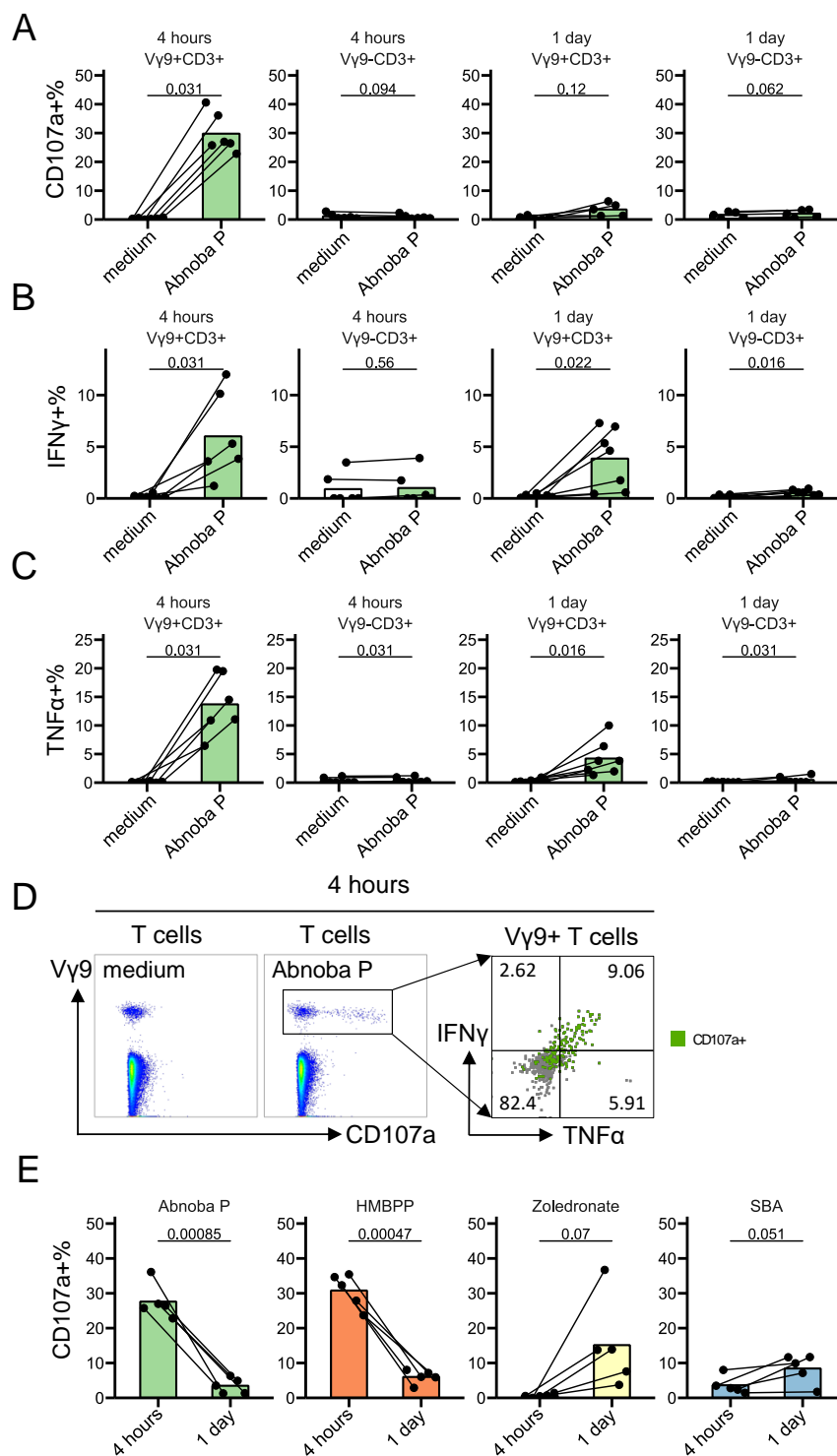


**Figure 2.** AbnobaViscum rapidly stimulate the release of cytotoxic granules and the production of IFN $\gamma$  and TNF $\alpha$  in V $\gamma$ 9V $\delta$ 2 T cells. (A–C) CD107a (A), IFN- $\gamma$  (B) and TNF- $\alpha$  (C) expression on V $\gamma$ 9+ T cells and V $\gamma$ 9- T cells after AbnobaViscum Pini (Abnoba P) stimulation. Lines connect the same subjects ( $n = 6$ ), bars indicate mean value. Values on the graphs indicate  $p$  values (obtained with the Wilcoxon signed-rank test). (D) Representative flow cytometry plots (4 h stimulation): the first two plots are gated on T cells (medium control on the left, Abnoba P on the right), the third plot is gated on V $\gamma$ 9+ T cells (Abnoba P), illustrating CD107a, IFN $\gamma$  and TNF $\alpha$  co-expression (E) Kinetics of CD107a expression on V $\gamma$ 9+ T cells by Abnoba P, HMBPP, zoledronate and sec-butylamine (SBA). Lines connect the same subjects ( $n = 5$ ), bars indicate mean values. Values on the graphs indicate  $p$  values (obtained with the paired  $T$ -test).



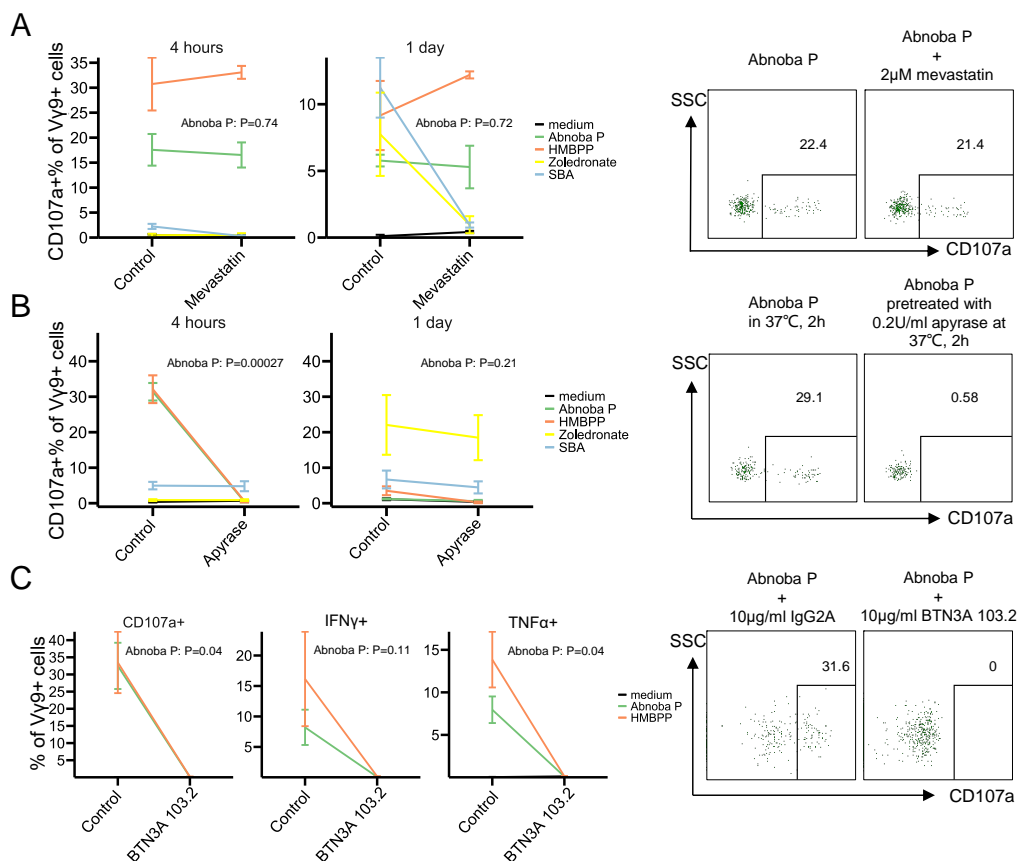


**Figure 3.** AbnobaViscum stimulation of Vγ9Vδ2 T cells is direct and BTN3A-dependent. **(A)** CD107a expression on Vγ9+ T cells upon mevastatin treatment within each stimulation. Lines connect the mean values between control and mevastatin treatment within the same stimulation, error bars show mean±sem ( $n = 3$ ). Representative flow cytometry plots after 4 h stimulation are on the right of the graphs (gate on CD3+Vγ9+ T cells). **(B)** CD107a expression on Vγ9+ T cells upon apyrase treatment within each stimulation. Lines connect the mean values between control and apyrase treatment within the same stimulation, error bars show mean±sem ( $n = 5$  for 4 h,  $n = 3$  for 1 day). Representative flow cytometry plots after 4 h stimulation are on the right of the graphs (gate on CD3+Vγ9+ T cells). **(C)** CD107a (left), IFNγ (middle), TNFα (right) expression in Vγ9+ T cells upon blocking BTN3A within each stimulation for 4 h. Lines connect the mean values between isotype control and BTN3A 103.2 mAb within the same stimulation, error bars show mean±sem ( $n = 3$ ). Representative CD107a stainings (4 h stimulation) after are on the right of the graphs (gate on CD3+Vγ9+ T cells). Values on the graphs indicate  $p$  values (obtained with paired  $T$ -test).

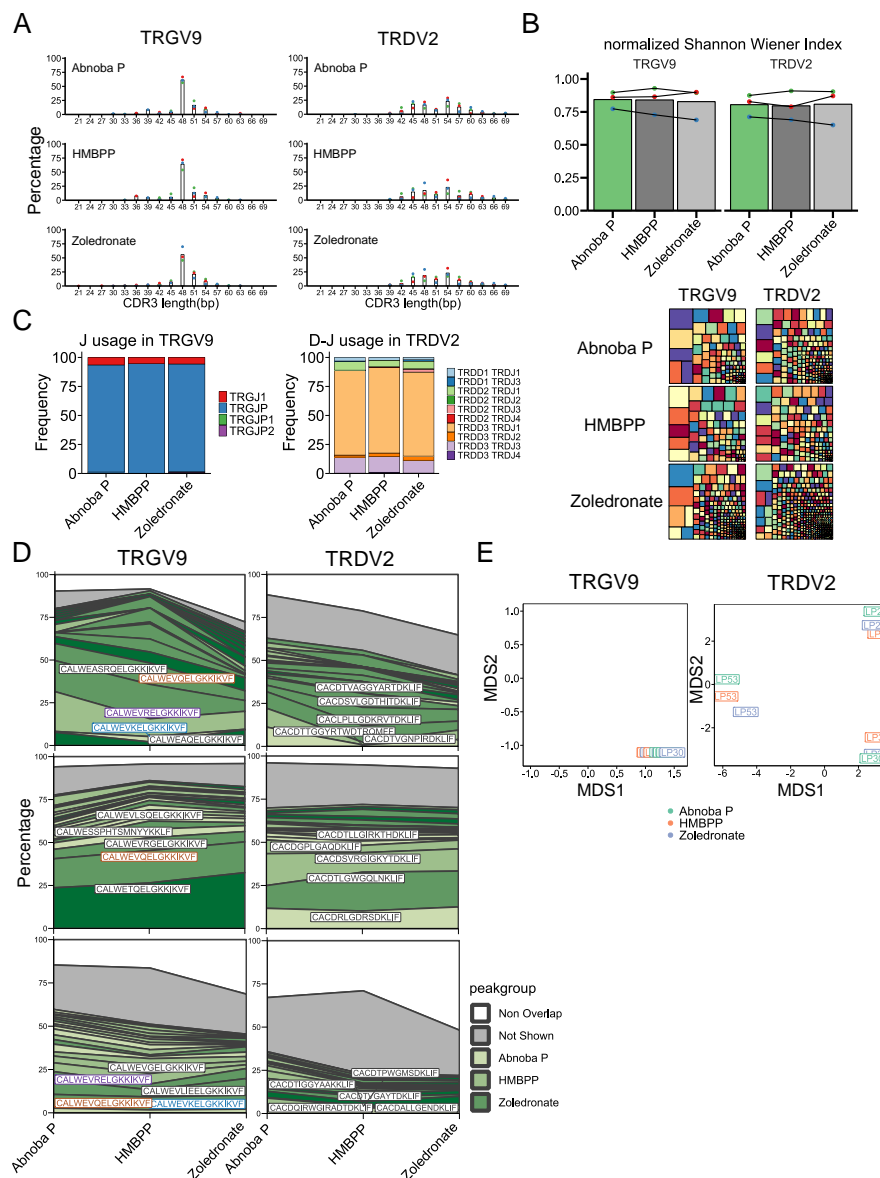


**Figure 4.** The AbnobaViscum-responsive  $V\gamma 9V\delta 2$  TCR repertoire is similar to the phosphoantigen-responsive repertoire. (A) Distribution of CDR3 length for TRGV9- and TRDV2-containing CDR3 sequences after expansion with the indicated  $V\gamma 9V\delta 2$  T cell stimulators. Each color of the dots represents the same subject, bar indicates mean percentage for each CDR3 length (expressed in nucleotides). (B) Diversity of TRGV9- and TRDV2- containing CDR3. Normalized Shannon Wiener index: each color of the dots represents the same subject, lines connect each subject, bars indicate mean value. Representative treemaps for the indicated stimulators are below the graphs: each small square represents a CDR3 sequence of which the size is related to the frequency of the sequence within the repertoire within each sample (rectangle colors are chosen randomly and do not match between plots). (C) Mean J gene segment usage in TRGV9-containing CDR3 (left) and mean D-J gene segment usage in TRDV2-containing CDR3 sequences (right) ( $n = 3$ ). (D) Sequence overlap between AP-, HMBPP- and zoledronate-induced expansions for TRGV9-containing CDR3 (left) and TRDV2-containing CDR3 (right). The top 20 sequences are filled with different green shades, the remaining overlapping sequences are indicated in grey and the non-overlapping sequences are in white. Top 5 shared sequences are provided on the plots for each subject: colored sequences occur in more than one subject while black sequences indicate unique sequences. (E) Multidimensional scaling analysis of TRGV9-containing CDR3 sequences (left) and TRDV2-containing CDR3 sequences (right). Colors indicate each expansion; the subject number is indicated within each small square.

#### 4. Discussion

Non-fermented mistletoe-extract drugs (AbnobaViscum) induced the specific expansion of V $\gamma$ 9V $\delta$ 2 T cells, the rapid release of their cytotoxic granules and production of IFN $\gamma$  and TNF $\alpha$ . All these features are known to be associated with anti-cancer activity [1,2]. AbnobaViscum has been shown to upregulate the expression of maturation markers on dendritic cells (DC), but failed to increase important cytokines such as IL-12p70 needed to stimulate and differentiate  $\alpha\beta$  T cells [31]. However, the promotion of IFN $\gamma$  production by V $\gamma$ 9V $\delta$ 2 T cells by AbnobaViscum may indirectly promote the full maturation of DC including IL-12p70 production [32–35] that is initiated by the direct DC-stimulation by mistletoe-derived lectins [31]. These fully mature DC could then in turn promote the development of (tumor) antigen-specific  $\alpha\beta$  T cell responses [35]. IL-17 production by  $\gamma\delta$  T cells has been associated with the promotion of tumor development [2,28], but we did not find evidence for significant production of this cytokine by V $\gamma$ 9V $\delta$ 2 T cells upon AbnobaViscum exposure.

The V $\gamma$ 9V $\delta$ 2 T cell response appeared to be specific to the type of preparation of the mistletoe extracts. Despite being derived from the same host trees (pine or apple tree), the bacterial-fermented extracts from Iscador did not result in the expansion of V $\gamma$ 9V $\delta$ 2 T cells. This was rather unexpected as the fermentation process could be a source of bacterial phosphoantigens [5,36] and thus indicates that these bacteria are not a source of V $\gamma$ 9V $\delta$ 2 T cell-activating phosphoantigens in mistletoe-extract drugs. Possibly, the fermentation process leads to a degradation of mistletoe-derived pyrophosphates and rather induce compounds that are stimulatory for NK cells. Indeed, it has been suggested that Iscador preparations are stimulatory while AbnobaViscum preparations are inhibitory for NK cells [15,18,37]. This is in line with our observation that Iscador induced higher CD69 expression on NK cells than AbnobaViscum. It is known that fermented and non-fermented mistletoe extracts can be very different in terms of their composition [38] and our recent metabolomics analysis on a series of mistletoe-extract drugs indicate that the composition of the extracts is much more dependent on the producer (company) than on the host tree (manuscript in preparation). Thus, the main immune cell target for fermented mistletoe extracts such as Iscador could be NK cells. The CD69 induction observed on V $\gamma$ 9V $\delta$ 2 T cells upon exposure towards Iscador extracts could therefore be secondary to NK cell activation and thus rather a bystander effect. While this bystander effect could be sufficient for the increased cell surface expression of the sensitive activation marker CD69, this effect may not be sufficient for the more robust signaling needed to induce expansion of the V $\gamma$ 9V $\delta$ 2 T cells [39] and thus provide a possible explanation why we did not observe any expansion of V $\gamma$ 9V $\delta$ 2 T cells upon exposure to Iscador extracts.

Alkylamines that are present in plants such as *sec*-butylamine have been shown to activate V $\gamma$ 9V $\delta$ 2 T cells indirectly by inhibiting the enzyme farnesyl pyrophosphate synthase resulting in the upregulation of endogenous phosphoantigens [8,10]. However, using approaches that verified the role of endogenous and exogenous phosphoantigens in the activation of V $\gamma$ 9V $\delta$ 2 T cells by AbnobaViscum, we show here that the activation is mediated directly and thus not depend on the intracellular accumulation of phosphoantigens. Our findings are in line with the observed sensitivity towards alkaline phosphatase of heat-treated mistletoe extract-induced  $\gamma\delta$  T cell expansion [26]. The absence of expansion without heat treatment [26] is likely due to the cytotoxic effects of the mistletoe extracts in longer term cell cultures needed to study proliferation. Indeed, we showed that the mistletoe-extract drugs as such (thus without heat treatment) are sufficient to stimulate V $\gamma$ 9V $\delta$ 2 T cells. In general, V $\gamma$ 9V $\delta$ 2 T cell-activating phosphoantigens can be derived from the mevalonate pathway or the non-mevalonate pathway, the latter also known as methylerythritol phosphate (MEP) pathway. Most organisms only use one of the two pathways for their isoprenoid synthesis. The MEP pathway is the one present in most (pathogenic) eubacteria and parasites of the phylum Apicomplexa, but it is absent from archaeobacteria, fungi, and animals, which synthesize their isoprenoids exclusively through the operation of the mevalonate pathway. By contrast, plants use both the MEP pathway and the mevalonate pathway for isoprenoid biosynthesis, although they are localized in different compartments: the MEP pathway is active in the plastids while the mevalonate pathway in the

cytosol [40]. These plastids are likely derived from once free-living bacteria by endosymbiosis [41,42]. *Viscum album* L, used for the generation of mistletoe-extract drugs, contains the gene expression profile of the enzymes needed for the MEP pathway [43]. HMBPP, a MEP pathway-derived V $\gamma$ 9V $\delta$ 2 T cell-activator, is up to 10,000 times more potent than the mevalonate pathway-derived V $\gamma$ 9V $\delta$ 2 T cell-activator IPP and is thus described as a main compound allowing V $\gamma$ 9V $\delta$ 2 T cells to sense cells infected with bacteria or parasites such as *Plasmodium* [5,44,45]. We propose that AbnobaViscum contains HMBPP or metabolites with a similar structure derived from the plastid-derived MEP pathway and thus that its administration mimics the presence of bacterial- or parasite-derived HMBPP resulting in the stimulation of V $\gamma$ 9V $\delta$ 2 T cells that are cross-reactive with cancer cells [46]. Since the AbnobaViscum-induced V $\gamma$ 9V $\delta$ 2 T cell stimulation was completely dependent on BTN3A, we propose that mistletoe-derived phosphoantigens such as HMBPP act in a direct and rapid manner via this ubiquitously expressed butyrophilin [6,47]. These phosphoantigens could act in concert with other mistletoe-derived compounds such as lectins (glycoproteins) and viscotoxins (polypeptides) targeting other immune cells such as DC and NK cells [31,48].

It has been recently described that both HMBPP and zoledronate stimulate polyclonal TCR responses as assessed by high-throughput sequencing of the V $\gamma$ 9V $\delta$ 2 TCR repertoire [30]. We wondered whether AbnobaViscum stimulated similar TCR responses as HMBPP and/or zoledronate, or whether it would act only on a restricted V $\gamma$ 9V $\delta$ 2 TCR repertoire as described for the tuberculosis vaccine BCG [49]. The AbnobaViscum-expanded V $\gamma$ 9V $\delta$ 2 TCR repertoire showed a high level of similarity with the HMBPP- and zoledronate-expanded repertoire at the level of CDR3 length, CDR3 diversity, and (D)J gene segment usage. Furthermore, the same top expanded TRGV9-associated CDR3 sequences could be found among AbnobaViscum-, HMBPP- and zoledronate- expanded TCR repertoires, that were highly shared among subjects (i.e., public). In contrast, the TRDV2-response was highly private: the expanded TCR repertoire was specific for each subject, confirming previous studies [30,50,51], but again the same top TRDV2-associated CDR3 sequences could be found in the AbnobaViscum-, HMBPP- and zoledronate-expanded TCR repertoires. Thus, AbnobaViscum appears to act on the same polyclonal V $\gamma$ 9V $\delta$ 2 TCR repertoire in adult peripheral blood as does HMBPP and IPP (upregulated by zoledronate), and not on a small subset of V $\gamma$ 9V $\delta$ 2 T cells. Despite significant recent progress regarding the molecular basis of phosphoantigen recognition by V $\gamma$ 9V $\delta$ 2 T cells, it is still not known to which molecular structures the CDR3 regions of both the TRGV9 and TRDV2 chains bind [52,53]. It remains thus unclear why the TRGV9 and TRDV2 repertoire of adult V $\gamma$ 9V $\delta$ 2 T cells, also after expansion with AbnobaViscum, are public and private respectively.

While bone targeting of aminobisphosphonates can be useful in the treatment of bone-related diseases, including cancer metastasis to the bones, this is rather a disadvantage for the treatment of most cancers that do not show bone metastasis. Furthermore, treatment with bisphosphonates such as zoledronate can lead to medication-related osteonecrosis of the jaw, a serious adverse reaction [54]. Thus, alternatives are being developed such as the ex-vivo expansion of V $\gamma$ 9V $\delta$ 2 T cells in order to re-infuse in cancer patients or the development of V $\gamma$ 9V $\delta$ 2 T cell-activators with potential improved pharmacokinetic properties [1,55,56]. However, these compounds are till now not administrated in vivo and the injection of expanded V $\gamma$ 9V $\delta$ 2 T cells have only been performed in the context of small phase 1/2 clinical trials [1]. In contrast, the administration of mistletoe-extract drugs is safe and about 500,000 cancer patients each year in Germany receive this treatment [14]. Our in vitro data regarding the stimulation of anti-cancer V $\gamma$ 9V $\delta$ 2 T cells by AbnobaViscum encourages the inclusion of these cells in future immunophenotyping studies upon AbnobaViscum treatment in vivo. Such immunophenotyping data and their possible correlation with clinical outcome will allow the stratification of cancer patients and are expected to provide insight into the controversial anti-cancer activities of mistletoe-extract drugs in cancer patients.

**Supplementary Materials:** The following are available online at <http://www.mdpi.com/2073-4409/9/6/1560/s1>, Figures S1–S4.

**Author Contributions:** Conceptualization, D.V.; methodology, L.M., S.P., C.S., F.S.; formal analysis, L.M., D.V.; investigation, L.M., S.P.; writing—original draft preparation, L.M., D.V.; writing—review and editing, S.P.; supervision, D.V. All authors have read and agreed to the published version of the manuscript.

**Funding:** L.M. is supported by the Chinese Scholarship Council (CSC), Fonds Van Buuren-Jaumotte-Demoulin and Fondation Rose et Jean Hoguet.

**Acknowledgments:** We thank Abnoba GmbH (Pforzheim, Germany) and Iscador AG (Arlesheim, Switzerland) for providing the mistletoe-extract herbal drugs and we thank ImCheck Therapeutics (Marseille, France) for providing the anti-BTN3A antibody clone 103.2.

**Conflicts of Interest:** The authors declare no conflict of interest.

## References

1. Sebestyén, Z.; Prinz, I.; Déchanet-Merville, J.; Silva-Santos, B.; Kuball, J. Translating gammadelta ( $\gamma\delta$ ) T cells and their receptors into cancer cell therapies. *Nat. Rev. Drug Discov.* **2020**, *19*, 169–184. [[CrossRef](#)] [[PubMed](#)]
2. Silva-Santos, B.; Mensurado, S.; Coffelt, S.B.  $\gamma\delta$  T cells: Pleiotropic immune effectors with therapeutic potential in cancer. *Nat. Rev. Cancer* **2019**, *19*, 392–404. [[CrossRef](#)] [[PubMed](#)]
3. Vermijlen, D.; Prinz, I. Ontogeny of Innate T Lymphocytes—Some Innate Lymphocytes are More Innate than Others. *Front. Immunol.* **2014**, *5*, 486. [[CrossRef](#)]
4. Fichtner, A.S.; Ravens, S.; Prinz, I. Human  $\gamma\delta$  TCR Repertoires in Health and Disease. *Cells* **2020**, *9*, 800. [[CrossRef](#)] [[PubMed](#)]
5. Eberl, M.; Hintz, M.; Reichenberg, A.; Kollas, A.K.; Wiesner, J.; Jomaa, H. Microbial isoprenoid biosynthesis and human gammadelta T cell activation. *FEBS Lett.* **2003**, *544*, 4–10. [[CrossRef](#)]
6. Boutin, L.; Scotet, E. Towards Deciphering the Hidden Mechanisms That Contribute to the Antigenic Activation Process of Human V $\gamma$ 9V $\delta$ 2 T Cells. *Front. Immunol.* **2018**, *9*, 828. [[CrossRef](#)]
7. Kobayashi, H.; Tanaka, Y. gammadelta T Cell Immunotherapy—A Review. *Pharmaceuticals* **2015**, *8*, 40–61. [[CrossRef](#)]
8. Bukowski, J.F.; Morita, C.T.; Brenner, M.B. Human gamma delta T cells recognize alkylamines derived from microbes, edible plants, and tea: Implications for innate immunity. *Immunity* **1999**, *11*, 57–65. [[CrossRef](#)]
9. Kamath, A.B.; Wang, L.; Das, H.; Li, L.; Reinhold, V.N.; Bukowski, J.F. Antigens in tea-beverage prime human Vgamma 2Vdelta 2 T cells in vitro and in vivo for memory and nonmemory antibacterial cytokine responses. *Proc. Natl. Acad. Sci. USA* **2003**, *100*, 6009–6014. [[CrossRef](#)]
10. Thompson, K.; Rojas-Navea, J.; Rogers, M.J. Alkylamines cause Vgamma9Vdelta2 T-cell activation and proliferation by inhibiting the mevalonate pathway. *Blood* **2006**, *107*, 651–654. [[CrossRef](#)]
11. Percival, S.S.; Bukowski, J.F.; Milner, J. Bioactive food components that enhance gammadelta T cell function may play a role in cancer prevention. *J. Nutr.* **2008**, *138*, 1–4. [[CrossRef](#)] [[PubMed](#)]
12. Holderness, J.; Hedges, J.F.; Daughenbaugh, K.; Kimmel, E.; Graff, J.; Freedman, B.; Jutila, M.A. Response of gammadelta T Cells to plant-derived tannins. *Crit. Rev. Immunol.* **2008**, *28*, 377–402. [[CrossRef](#)]
13. Kalyan, S.; Kabelitz, D. Defining the nature of human gammadelta T cells: A biographical sketch of the highly empathetic. *Cell Mol. Immunol.* **2013**, *10*, 21–29. [[CrossRef](#)] [[PubMed](#)]
14. Horneber, M.A.; Bueschel, G.; Huber, R.; Linde, K.; Rostock, M. Mistletoe therapy in oncology. *Cochrane Database Syst. Rev.* **2008**, *2008*, CD003297. [[CrossRef](#)] [[PubMed](#)]
15. Bar-Sela, G. White-Berry Mistletoe (*Viscum album* L.) as complementary treatment in cancer: Does it help? *Eur. J. Integr. Med.* **2011**, *3*, e55–e62. [[CrossRef](#)]
16. Matthes, H.; Thronicke, A.; Hofheinz, R.-D.; Baars, E.; Martin, D.; Huber, R.; Breitzkreuz, T.; Bar-Sela, G.; Galun, D.; Schad, F.; et al. Statement to an Insufficient Systematic Review on *Viscum album* L. Therapy. *Evid. Based Complement. Altern. Med.* **2020**, *2020*, 7091039. [[CrossRef](#)]
17. PDQ Integrative, Alternative, and Complementary Therapies Editorial Board. Mistletoe Extracts (PDQ®): Health Professional Version. In *PDQ Cancer Information Summaries*; National Cancer Institute (US): Bethesda, MD, USA, 2019.
18. Grudzien, M.; Rapak, A. Effect of Natural Compounds on NK Cell Activation. *J. Immunol. Res.* **2018**, *2018*, 4868417. [[CrossRef](#)]
19. Oei, S.L.; Thronicke, A.; Schad, F. Mistletoe and Immunomodulation: Insights and Implications for Anticancer Therapies. *Evid. Based Complement. Altern. Med.* **2019**, *2019*, 1–6. [[CrossRef](#)]



20. Harly, C.; Guillaume, Y.; Nedellec, S.; Peigne, C.M.; Monkkonen, H.; Monkkonen, J.; Li, J.; Kuball, J.; Adams, E.J.; Netzer, S.; et al. Key implication of CD277/butyrophilin-3 (BTN3A) in cellular stress sensing by a major human gammadelta T-cell subset. *Blood* **2012**, *120*, 2269–2279. [[CrossRef](#)]
21. Morita, C.T.; Parker, C.M.; Brenner, M.B.; Band, H. TCR usage and functional capabilities of human gamma delta T cells at birth. *J. Immunol.* **1994**, *153*, 3979–3988.
22. Tieppo, P.; Papadopoulou, M.; Gatti, D.; McGovern, N.; Chan, J.K.Y.; Gosselin, F.; Goetgeluk, G.; Weening, K.; Ma, L.; Dauby, N.; et al. The human fetal thymus generates invariant effector  $\gamma\delta$  T cells. *J. Exp. Med.* **2020**, *217*, e20190580. [[CrossRef](#)] [[PubMed](#)]
23. Bolotin, D.A.; Poslavsky, S.; Mitrophanov, I.; Shugay, M.; Mamedov, I.Z.; Putintseva, E.V.; Chudakov, D.M. MiXCR: Software for comprehensive adaptive immunity profiling. *Nat. Methods* **2015**, *12*, 380–381. [[CrossRef](#)] [[PubMed](#)]
24. Shugay, M.; Bagaev, D.V.; Turchaninova, M.A.; Bolotin, D.A.; Britanova, O.V.; Putintseva, E.V.; Pogorelyy, M.V.; Nazarov, V.I.; Zvyagin, I.V.; Kirgizova, V.I.; et al. VDJtools: Unifying Post-analysis of T Cell Receptor Repertoires. *PLoS Comput. Biol.* **2015**, *11*, e1004503. [[CrossRef](#)] [[PubMed](#)]
25. Wickham, H. *ggplot2*; Springer: New York, NY, USA, 2009; ISBN 978-0-387-98140-6.
26. Fischer, S.; Scheffler, A.; Kabelitz, D. Activation of human gamma delta T-cells by heat-treated mistletoe plant extracts. *Immunol. Lett.* **1996**, *52*, 69–72. [[CrossRef](#)]
27. Ma, Y.; Aymeric, L.; Locher, C.; Mattarollo, S.R.; Delahaye, N.F.; Pereira, P.; Boucontet, L.; Apetoh, L.; Ghiringhelli, F.; Casares, N.; et al. Contribution of IL-17-producing gamma delta T cells to the efficacy of anticancer chemotherapy. *J. Exp. Med.* **2011**, *208*, 491–503. [[CrossRef](#)] [[PubMed](#)]
28. Van Hede, D.; Polese, B.; Humblet, C.; Wilharm, A.; Renoux, V.; Dortu, E.; de Leval, L.; Delvenne, P.; Desmet, C.J.; Bureau, F.; et al. Human papillomavirus oncoproteins induce a reorganization of epithelial-associated  $\gamma\delta$  T cells promoting tumor formation. *Proc. Natl. Acad. Sci. USA* **2017**, *114*, E9056–E9065. [[CrossRef](#)]
29. Wang, H.; Sarikonda, G.; Puan, K.J.; Tanaka, Y.; Feng, J.; Giner, J.L.; Cao, R.; Monkkonen, J.; Oldfield, E.; Morita, C.T.; et al. Indirect stimulation of human Vgamma2Vdelta2 T cells through alterations in isoprenoid metabolism. *J. Immunol.* **2011**, *187*, 5099–5113. [[CrossRef](#)]
30. Fichtner, A.S.; Bubke, A.; Rampoldi, F.; Wilharm, A.; Tan, L.; Steinbrück, L.; Schultze-Florey, C.; von Kaisenberg, C.; Prinz, I.; Herrmann, T.; et al. TCR repertoire analysis reveals phosphoantigen-induced polyclonal proliferation of V $\gamma$ 9V $\delta$ 2 T cells in neonates and adults. *J. Leukoc. Biol.* **2020**. [[CrossRef](#)]
31. Steinborn, C.; Klemm, A.M.; Sanchez-Campillo, A.-S.; Rieger, S.; Scheffen, M.; Sauer, B.; Garcia-Käuffer, M.; Urech, K.; Follo, M.; Ücker, A.; et al. *Viscum album* neutralizes tumor-induced immunosuppression in a human in vitro cell model. *PLoS ONE* **2017**, *12*, e0181553. [[CrossRef](#)]
32. Ismaili, J.; Oslislagers, V.; Poupot, R.; Fournie, J.J.; Goldman, M. Human gamma delta T cells induce dendritic cell maturation. *Clin. Immunol.* **2002**, *103*, 296–302. [[CrossRef](#)]
33. Conti, L.; Casetti, R.; Cardone, M.; Varano, B.; Martino, A.; Belardelli, F.; Poccia, F.; Gessani, S. Reciprocal activating interaction between dendritic cells and pamidronate-stimulated gammadelta T cells: Role of CD86 and inflammatory cytokines. *J. Immunol.* **2005**, *174*, 252–260. [[CrossRef](#)] [[PubMed](#)]
34. Devilder, M.C.; Maillet, S.; Bouyge-Moreau, I.; Donnadiou, E.; Bonneville, M.; Scotet, E. Potentiation of antigen-stimulated V gamma 9V delta 2 T cell cytokine production by immature dendritic cells (DC) and reciprocal effect on DC maturation. *J. Immunol.* **2006**, *176*, 1386–1393. [[CrossRef](#)]
35. Fiore, F.; Castella, B.; Nuschak, B.; Bertieri, R.; Mariani, S.; Bruno, B.; Pantaleoni, F.; Foglietta, M.; Boccadoro, M.; Massaia, M. Enhanced ability of dendritic cells to stimulate innate and adaptive immunity on short-term incubation with zoledronic acid. *Blood* **2007**, *110*, 921–927. [[CrossRef](#)] [[PubMed](#)]
36. Micozzi, M.S. Natural products in cancer care and treatment. In *Complementary and Integrative Medicine in Cancer Care and Prevention*; Springer Publishing Company: New York, NY, USA, 2006; pp. 243–280.
37. Lee, S.J.; Son, Y.-O.; Kim, H.; Kim, J.-Y.; Park, S.-W.; Bae, J.-H.; Kim, H.H.; Lee, E.-Y.; Chung, B.-S.; Kim, S.-H.; et al. Suppressive effect of a standardized mistletoe extract on the expression of activatory NK receptors and function of human NK cells. *J. Clin. Immunol.* **2007**, *27*, 477–485. [[CrossRef](#)] [[PubMed](#)]
38. Ribéreau-Gayon, G.; Jung, M.-L.; Di Scala, D.; Beck, J.-P. Comparison of the Effects of Fermented and Unfermented Mistletoe Preparations on Cultured Tumor Cells. *Oncology* **1986**, *43*, 35–41. [[CrossRef](#)]

39. Vermijlen, D.; Ellis, P.; Langford, C.; Klein, A.; Engel, R.; Willmann, K.; Jomaa, H.; Hayday, A.C.; Eberl, M. Distinct cytokine-driven responses of activated blood gamma delta T cells: Insights into unconventional T cell pleiotropy. *J. Immunol.* **2007**, *178*, 4304–4314. [[CrossRef](#)]
40. Rodríguez-Concepción, M.; Boronat, A. Elucidation of the methylerythritol phosphate pathway for isoprenoid biosynthesis in bacteria and plastids. A metabolic milestone achieved through genomics. *Plant Physiol.* **2002**, *130*, 1079–1089. [[CrossRef](#)]
41. Archibald, J.M. Genomic perspectives on the birth and spread of plastids. *Proc. Natl. Acad. Sci. USA* **2015**, *112*, 10147–10153. [[CrossRef](#)]
42. Sibbald, S.J.; Archibald, J.M. Genomic insights into plastid evolution [published online ahead of print, 13 May 2020]. *Genome Biol. Evol.* **2020**, evaa096. [[CrossRef](#)]
43. Xie, W.; Adolf, J.; Melzig, M.F. Identification of *Viscum album* L. miRNAs and prediction of their medicinal values. *PLoS ONE* **2017**, *12*, e0187776. [[CrossRef](#)]
44. Eberl, M.; Roberts, G.W.; Meuter, S.; Williams, J.D.; Topley, N.; Moser, B. A rapid crosstalk of human gamma delta T cells and monocytes drives the acute inflammation in bacterial infections. *PLoS Pathog.* **2009**, *5*, e1000308. [[CrossRef](#)] [[PubMed](#)]
45. Davey, M.S.; Lin, C.Y.; Roberts, G.W.; Heuston, S.; Brown, A.C.; Chess, J.A.; Toleman, M.A.; Gahan, C.G.; Hill, C.; Parish, T.; et al. Human neutrophil clearance of bacterial pathogens triggers anti-microbial gamma delta T cell responses in early infection. *PLoS Pathog.* **2011**, *7*, e1002040. [[CrossRef](#)] [[PubMed](#)]
46. Riganti, C.; Massaia, M.; Davey, M.S.; Eberl, M. Human  $\gamma\delta$  T-cell responses in infection and immunotherapy: Common mechanisms, common mediators? *Eur. J. Immunol.* **2012**, *42*, 1668–1676. [[CrossRef](#)]
47. Nerdal, P.T.; Peters, C.; Oberg, H.-H.; Zlatev, H.; Lettau, M.; Quabius, E.S.; Sousa, S.; Gonnermann, D.; Auriola, S.; Olive, D.; et al. Butyrophilin 3A/CD277-Dependent Activation of Human  $\gamma\delta$  T Cells: Accessory Cell Capacity of Distinct Leukocyte Populations. *J. Immunol. Baltim. Md 1950* **2016**, *197*, 3059–3068. [[CrossRef](#)] [[PubMed](#)]
48. Tabiasco, J.; Pont, F.; Fournié, J.-J.; Vercellone, A. Mistletoe viscotoxins increase natural killer cell-mediated cytotoxicity. *Eur. J. Biochem.* **2002**, *269*, 2591–2600. [[CrossRef](#)] [[PubMed](#)]
49. Spencer, C.T.; Abate, G.; Blazevic, A.; Hoft, D.F. Only a subset of phosphoantigen-responsive gamma delta 2 T cells mediate protective tuberculosis immunity. *J. Immunol.* **2008**, *181*, 4471–4484. [[CrossRef](#)] [[PubMed](#)]
50. Papadopoulou, M.; Tieppo, P.; McGovern, N.; Gosselin, F.; Chan, J.K.Y.; Goetgeluk, G.; Dauby, N.; Cogan, A.; Donner, C.; Ginhoux, F.; et al. TCR Sequencing Reveals the Distinct Development of Fetal and Adult Human V $\gamma$ 9V $\delta$ 2 T Cells. *J. Immunol.* **2019**, *203*, 1468–1479. [[CrossRef](#)]
51. Davey, M.S.; Willcox, C.R.; Hunter, S.; Kasatskaya, S.A.; Remmerswaal, E.B.M.; Salim, M.; Mohammed, F.; Bemelman, F.J.; Chudakov, D.M.; Oo, Y.H.; et al. The human V $\delta$ 2+ T-cell compartment comprises distinct innate-like V $\gamma$ 9+ and adaptive V $\gamma$ 9– subsets. *Nat. Commun.* **2018**, *9*, 1–14. [[CrossRef](#)]
52. Herrmann, T.; Fichtner, A.S.; Karunakaran, M.M. An Update on the Molecular Basis of Phosphoantigen Recognition by V $\gamma$ 9V $\delta$ 2 T Cells. *Cells* **2020**, *9*, 1433. [[CrossRef](#)]
53. Vyborova, A.; Beringer, D.X.; Fasci, D.; Karaiskaki, F.; van Diest, E.; Kramer, L.; de Haas, A.; Sanders, J.; Janssen, A.; Straetemans, T.; et al.  $\gamma$ 9 $\delta$ 2T cell diversity and the receptor interface with tumor cells [published online ahead of print, 2 June 2020]. *J. Clin. Investig.* **2020**. [[CrossRef](#)]
54. Beth-Tasdogan, N.H.; Mayer, B.; Hussein, H.; Zolk, O. Interventions for managing medication-related osteonecrosis of the jaw. *Cochrane Database Syst. Rev.* **2017**, *10*, CD012432. [[CrossRef](#)] [[PubMed](#)]
55. Hsiao, C.-H.C.; Lin, X.; Barney, R.J.; Shippy, R.R.; Li, J.; Vinogradova, O.; Wiemer, D.F.; Wiemer, A.J. Synthesis of a phosphoantigen prodrug that potently activates V $\gamma$ 9V $\delta$ 2 T-lymphocytes. *Chem. Biol.* **2014**, *21*, 945–954. [[CrossRef](#)] [[PubMed](#)]
56. Kilcollins, A.M.; Li, J.; Hsiao, C.-H.C.; Wiemer, A.J. HMBPP Analog Prodrugs Bypass Energy-Dependent Uptake To Promote Efficient BTN3A1-Mediated Malignant Cell Lysis by V $\gamma$ 9V $\delta$ 2 T Lymphocyte Effectors. *J. Immunol.* **2016**, *197*, 419–428. [[CrossRef](#)] [[PubMed](#)]

